Floral development of monoecious *Pseuduvaria trimera* (Annonaceae) and comparative morphology and structure of its stamens and indehiscent staminodes

Guifang Yang[1, 2]; Fengxia Xu[1]*

1. Key Laboratory of Plant Resources Conservation and Sustainable Utilization, South China Botanical Garden, Chinese Academy of Sciences, 723 Xingke Road, Tianhe District, Guangzhou, Guangdong 510650, China

2. University of Chinese Academy of Sciences, Beijing 100049, China

*Corresponding author: Feng-Xia Xu Email: xfx@scbg.ac.cn

Keywords: floral development; monoecy; indehiscent staminode; *Pseuduvaria trimera*; morphology; anatomy

Abstract

Premise of research. Comparative development of staminate and pistillate flowers of *Pseuduvaria trimera* (Annonaceae) is firstly investigated to understand its sexual differentiation and developmental processes of flowers. Comparisons of morphological and anatomical features between mature stamens and staminodes are also described, in order to clarify the mode of anther dehiscence and understand the mechanism underlying the sterility of the staminodes.

Methodology. Flowers at different developmental stages and mature stamens and

staminodes were examined with SEM and light microscopy.

Pivotal results. Flowers have complex whorled phyllotaxis as in other Annonaceae, with double positions in the outmost whorl of reproductive organs and variable stamen and carpel organ numbers per whorl. The stomium region of each theca is composed of the septum and stomium. The septum and stomium cells of stamens could be degenerated developmentally, facilitating anther opening, whereas those of staminodes maintain intact, forming indehiscent anthers.

Conclusions. The developmental data suggest that staminate flower is unisexual from inception, while pistillate flower is morphologically hermaphroditic. The morphologically hermaphroditic flowers are nevertheless functionally pistillate as the anthers are indehiscent, and the structural andromonoecy of *P. trimera* actually functions as monoecy. The mechanism underlying the sterility of the indehiscent staminodes and delayed dehiscent outer stamens might be effective in promoting xenogamy. The occurrence of staminode is closely correlated with the acquisition and evolution of functional unisexual flowers in the genus *Pseuduvaria*.

Introduction

The Annonaceae is an early-divergent angiosperm family comprising 112 genera and about 2440 species (Couvreur et al. 2011). The majority of Annonaceae genera

have hermaphroditic flowers, but unisexual flowers occur in several disparate lineages and have evolved independently in these lineages (Saunders 2010). Plants from most of these genera are structurally androdioecious or andromonoecious, and only a few have solely unisexual flowers, for instance, the genus *Pseuduvaria* (Su and Saunders 2006; Su et al. 2008). In *Pseuduvaria*, the interpretations of floral sex expression were based on assumptions of reproductive organ functionality, including the fertility of stamens in hermaphroditic or staminate flowers and the sterility of staminodes in pistillate flowers. The sterility of these staminodes was due either to lack of any pollen grain or occurrence of sterile pollen grains only, according to morphological observation from herbarium materials (Su and Saunders 2006). However, the pollen grains from both hermaphroditic flowers and staminate flowers in *Pseuduvaria mulgraveana* were proved to be equally viable via vivo and vitro pollen germination tests, but the stamens from hermaphroditic flowers become sterile as the anther dehiscence was delayed until after the departure of pollinators (Pang et al. 2013). The present observation on *P. trimera* shows that pollen grains from stamens in staminate flowers and staminodes in pistillate flowers are similar in morphology. Only based on morphology from herbarium specimens to interpret the sterility of staminodes seems not supportable, and the determination of floral sex expression based on the

assumptions is required for a reappraisal in this genus. Comparatively anatomical and morphological analyses on fresh stamens and staminodes are therefore essential for understanding the process on the sterility of staminodes and the mechanism to acquire unisexual flowers in *Pseuduvaria*. Moreover, the information on floral development is crucial for determining the morphologically developmental types of unisexual flowers and understanding the evolutionary origins of the developmental patterns in unisexual flowers. However, except for stamen development in staminate flowers in *P. indochinensis* (synonym of *P. trimera*: Xu and Ronse De Craene 2010), detailed floral developmental and structural investigations of unisexual flowers in this genus and Annonaceae have been very scarce. This present study aims to provide detailed description of floral development in both staminate and pistillate in *P. trimera*, with emphasis on the crucial stage when the first morphological differences appear between staminate and pistillate flowers and the determination of developmental patterns. In particular, comparative morphological and anatomical analyses of stamens and staminodes at anthesis are firstly investigated, in order to understand the processes of anther dehiscence and the mechanism underlying the sterility of the well-developed staminode in *Pseuduvaria*.

Material and Methods

Both fresh staminate and pistillate inflorescences at a range of different developmental stages were collected and fixed immediately in FAA (70% alcohol, formaldehyde and glacial acetic acid in a ratio of 90: 5: 5) from December 2012 to February 2014, from the trees cultivated at the Xishuangbanna Tropical Botanical Garden, the Chinese Academy of Sciences.

For scanning electron microscopic observation the specimens were carefully dissected in 70% ethanol under a dissecting microscope. After dissection, samples (floral buds, stamens, and staminodes) were dehydrated through graded acetone series and critical point dried. Materials were then mounted on stubs, coated with gold using JFC-1600 Auto Fine Coater (JEOL, Tokyo, Japan), and observed under a JSM-6360LV SEM (JEOL, Tokyo, Japan) scanning electron microscope, operated at 15 kV. The pollen tetrads were directly mounted on stubs, coated with gold, and observed under the SEM, after removal from the stamens and staminodes.

For light microscope observations, dissected stamens and staminodes at anthesis were transferred to 2% glutaraldehyde in 0.1M phosphate buffer at pH 7.2-7.4 overnight at 4℃. Samples were dehydrated in an ethanol series, embedded in Spurr Resin, and sectioned at 2 μm using a rotary microtome. Sections were stained with

Toluidine Blue and observed under a light microscope (Leica, DM5500B). Reference material is kept at South China Botanical Garden (IBSC).

Results

Floral morphology

Two different floral morphs are present in *P. trimera*, i.e. structurally hermaphroditic flowers with both carpels and staminodes and staminate flowers lacking pistillodes co-occur at the same tree. Inflorescences are clustered on branches. Each inflorescence consists of numerous flowers (all of the same gender), but only one undergoes anthesis at any time, followed by a second flower with outer petal opening, and by several other closed buds differing in size and in pedicel length (fig. 1*A*).

Each flower has a stable trimerous perianth, comprising one whorl of three sepals and two whorls of petals. The sepals are small and free. The triangular outer petals become strongly reflexed, forming three lateral apertures between the claws of the inner petals, whilst the inner petals lack glands and are apically coherent over the reproductive parts, forming an enclosed mitriform floral chamber. The lateral apertures, together with the reflexed outer petals, act as valves allowing the pollinators to gain access to the mitriform floral chamber (fig. 1*B*, 1*E*). The mitriform

inner petal whorl abscises as a whole, whereas the outer petal whorl persists (fig. 1*D*, 1*G*). Each pistillate flower has 9–15 free carpels and an outermost whorl of 1–6 staminodes, opposite the outer petals. Occasionally, pistillate flower with 13 staminodes or even no staminode is also observed. Staminodes are indehiscent and persistent when the stigmas become dark and look like dry and shrunk, and the inner petals are abscised (fig. 1*C*, 1*D*). Each staminate flower contains 46–56 firmly packed stamens (fig. 1*E*). The androecium matures and dehisces centrifugally, with stamens at the center dehiscing and shedding before those at the margin (fig. 1*F*).

Floral ontogeny

Developmental stages shared by pistillate and staminate flowers

Some early developmental stages are common on pistillate and staminate flowers, starting from the appearance of bract primordium to the initiation of the first whorl of reproductive organs. A bract primordium appears encircling the floral apex (fig. 2*A*). After initiation of the first subtending bract primordium, the apical meristem becomes higher and another bract primordium is immediately initiated, subtending the floral apex and opposite the first one (fig. 4*A*). The floral apex is initially circular (fig. 4*A*) but gradually becomes triangular after the first whorl of three sepal primordia is

successively initiated. The first sepal primordium is slightly larger than the other two and positioned opposite the bract (fig. 2*B*–2*D*, 4*B*). The second whorl of the three outer petal primordia is initiated simultaneously at the tips of the three angles of the triangular floral apex, alternating with the sepal primordia (fig. 2*E*, 4*B*). The initiation of the third whorl of the three inner petal primordia is similar to the outermost sepal whorl, with one of them arising slightly earlier than the other two, and they are in alternation with the outer petal whorl. After the completion of the perianth initiation, the remaining floral apex becomes more or less hexagonal (fig. 2*F*, 4*C*). All the petal primordia are enlarged and become slightly curved as they grow, and they completely cover the remaining floral apex in later development. When hair appears on the back of the outer petals, three pairs of stamen primordia (in staminate flowers) or staminode primordia (in pistillate flowers) arise simultaneously on the hexagonal floral apex, in a position opposite the outer petals (fig. 2*G*, *H*).

Development of the gynoecium and staminodes in pistillate flower

Following the initiation of a first whorl built by staminode primordia, a whorl of 8–12 carpel primordia arises simultaneously around the margin of the remaining floral apex. The carpel primordia are approximately hemispherical, differing slightly in size, while the outer staminode primordia are uniformly oblate (fig. 2*I*–2*M*). When a

ventral depression develops in the middle of the first whorl of carpel primordia, a second whorl of 3–4 carpel primordia arises at the center of floral apex (fig. 3*A*–3*C*). Immediately after the second whorl carpel primordia initiation, all carpel primordia become horseshoe-shaped primordia (fig. 3*D*). Then, the central depression deepens unilaterally into a narrow slit by growth of marginal tissue. At this stage, hair develops at the residual floral apex and between the carpels (fig. 3*D*, 3*E*). When hair become long and beyond carpels, the apical part develops into a stigma head, and the basal part expands horizontally into a bulging ovary (fig. 3*F*, 3*H*). At maturity, the whole carpel grows into a plicate structure that lacks a true style, with the stigma head differentiating into a folded and funnel-shaped stigmatic structure. At this time, the ovaries are covered with clusters of hairs (fig. 3*I*). The carpels occupy the entire floral apex ultimately.

After the first whorl of carpel primordia initiation, the number of staminode primordia becomes 3–6, only in one flower bud were observed 13 staminode primordia, appearing either in double or single positions, opposite the outer petals (fig. 2*I*–2*L*). The staminode primordia become large and differentiate into dorsal microsporagia, when the carpel primordia become large and have undergone morphological differentiation with an apical stigma head and a lower ovary. At this

stage, hairs also appear dense and long between the carpels (fig. 3*F*, 3*G*).

Development of the androecium in staminate flower

After the first whorl of three paired stamen primordia appearing, more stamen primordia start to initiate along the sides of the hexagonal floral apex centripetally in a relatively rapid succession with little indications of a sequence pattern (fig. 4*D*–4*G*). During this stage, hair develops on the back of the inner petals and the floral apex becomes greatly higher, comparing with the previous stages of perianth primordium initiating. Towards the top of the floral apex, initiation of the remaining stamen primordia appears in whorled but with an inconstant merism, varying from a hexamerous (fig. 4*H*) to a trimerous whorl (fig. 4*I*), ending with the single one (fig. 4*J*), as the availability of floral apex for initiation becomes limited. Subsequently, all stamen primordia quickly differentiate dorsal microsporangia and grow into a compact androecium (fig. 4*M*), indicated by the appearance of the hairs between stamen primordia (fig. 4*K*, 4*L*). Any evidence of carpel primordia initiation or abortion could not be found during the whole developmental process.

Morphology and structure of the stamen and staminode at anthesis

Morphology and structure of the stamen

The mature stamens are flat and exhibit pronouncedly extrorse microsporangia,

containing tetrahedral, isobilateral, decussate, and T-shaped tetrads with microrugulate ornamentation of exine. Each stamen has a continuation of the connective tissue extending over the dorsal fertile tissues, forming a broad, flatted connective appendage (fig. 5*A*–5*C*). Stamens in the inner whorls of the androecium contain four long parallel microsporangia, situated in two pairs, and each pair differs slightly in length, with the outer one a little longer than the inner one (fig. 5*A*). While in the outermost whorl stamen, the number of the microsporangia is reduced to three sometime and the length of the microsporangia appears about one half of the inner stmens (fig. 5*B*, 5*C*). The outermost whorl of stamens is also broader than the others (fig. 5*B*, 5*C*).

Stamens in the inner whorls and the outermost whorl of androecium show the same overall structural organization. In cross sections, each anther is served by a single vascular bundle at the center of the connective tissue. The anther wall comprises an epidermis and an endothecium layer. Endothecium is restricted to the microsporangia, which have a more or less rectangle shape and conspicuous U-shaped wall thickenings. Besides, an endothecial-like hypodermis layer surrounding the lateral portions of the microsporangia and the connective, together with the endothecium produce a ring that encircles the whole anther. The outermost single

epidermis layer cells are greatly smaller than those of the neighboring endothecium and endothecial-like hypodermis layer, surrounding the whole anther tissues. They are continuous at the region adjacent to endothecial-like hypodermis layer and discontinuous at the region close to the endothecium cells (fig. 6*A*–6*M*). The stomium region between the paired microsporangia is composed of a septum layer close to the connective tissue and a stomium with 1–3 cells continuing with the epidermis (fig. 6*B*, 6*L*). These two layers of cells are very small comparing with the cells of neighboring connective and anther wall. Unlike the endothecium and epidermis, they do not undergo thickening. The septum cells close to the locule firstly break down (fig. 6*D*, 6*J*), and later the midlle ones either break down as well, or completely separate from the connective tissues, together with the stomium cells, endothecium, and the epidermis, forming one large pollen locule (fig. 6*E*), immediately followed by the disruption of the remaining septum and stomium cells (fig. 6*G*). Following these cells breakage, the anthers dehisce extrorsely and release the tetrad pollen grains (fig. 6*G*, 6*H*). In particular, the stomium region of the single microsporangium of the outermost stamens develops two layers of septum cells between the connective tissue and the epidermis, but they broke down to release the tetrad pollen grains in the same pattern as the inner stamens (fig. 6*M*).

Morphology and structure of the staminode

The microsporangia of staminode contain tetrahedral, isobilateral, decussate, and T-shaped tetrads with microrugulate ornamentation of exine (fig. 5*L*, 5*M*). Like the outermost stamens, the number of the microsporangium is frequently reduced to three or two, and the sizes of the paired microsporangia differ greatly, with the outer one being larger than the inner (fig. 5*D*–5*I*). Besides, some staminodes do not dehisce but the connectives of them become greatly shrunk (fig. 5*H*, 5*I*). In cross sections, the stomium region between the paired microsporangia consists of a septum and a stomium. The former contains two layers of compact cells, close to the connective tissue; whereas the latter comprises 1–3 cells, continuing with the epidermis (fig. 7*A*, 7*B*, 7*D*–7*G*). Both the septum and stomium cells remain intact and the microsporangia keep indehiscent at anthesis (fig. 7*D*, 7*E*, 7*H*). The stomium region of the single microsporangium develops no septum cells (fig. 7*C*).

Discussion

Floral phyllotaxis

Despite the developmental patterns of floral organs are highly variable in Annonaceae, the family appears uniform in its simple or complex, or irregular whorled floral phyllotaxis, with double positions in the first stamen whorl, and almost

uniform in its completely plicate carpels (Ronse De Craene and Smets 1990; Endress and Doyle 2007; Xu and Ronse De Craene 2010; Endress and Armstrong 2011; this study). Endress and Armstrong (2011) classified floral phyllotaxis in Annonaceae into three types in terms of the correlation between floral organ number and phyllotaxis, simple regular whorls (with a low number of floral organs), complex whorls (with a medium number of floral organs), and irregular phyllotaxis (with numerous stamens and carpels). In this study, the pistillate flower has variable organ number per whorl ranging from 3 (perianth whorl), 6 (staminode whorl), 8–12 (the first carpel whorl), to 3–4 (the second carpel whorl), which could be considered as complex whorled phyllotaxis. In the case of the staminate flower, the phyllotaxis of the androecium is more complicated compared to the pistillate flower. The initiation of the first and ultimate three whorls of stamens is whorled, while the remaining stamens are initiated in a rapid succession with undetectable sequence pattern. All stamens form a whorled arrangement at maturity. It suggests that the floral phyllotaxis of the staminate flower is also classified as complex whorls.

Bracts development

In both pistillate and staminate flowers of *P. trimera*, two bracts are observed to subtend the flower during the entire floral development and could presumably protect

the floral meristem in their early stages of differentiation. Two sheathing bracts also proposed in Himantandraceae by Endress (2003). However, one sheathing bract was reported in *Anaxagorea* (Endress and Armstrong 2011), as well as in *Myristica* (Armstrong and Tucker 1986), Eupomatiaceae and Magnoliaceae (Endress 2003; Kim et al. 2005). In the other genera of Annonaceae, the sheathing bract has not been reported. From the phylogenetic analysis, it appears that the presence of a sheathing bract, as present in the basal genus *Anaxagorea* of Annonaceae which has hermaphrodictic flowers, might be primitive in the family, and two sheathing bracts as in the unisexual flowers of *P. trimera* are therefore probably derived.

Morpho-anatomical features of stamens and staminodes

Although both stamens and staminodes contain dorsal microsporangia, with the similarity in tetrads shapes, size, and microrugulate ornamentation of exine, and have the same overall organization of anther structure, the length and number of microsporangia decrease greatly both in the outer stamens and staminodes, comparing with the inner stamens. In the outer stamens and other fertile stamens, the stomium region in anther notch is composed of a layer of specialized septum cells and 1–3 modified epidermal cells (stomium). This stomium region structure is similar to the other flowering plants, including *Arabidopsis thaliana* (Sanders et al. 1999), rice

(Matsui et al. 1999), maize (Keijzer et al. 1996), and members of the Solanaceae, including tobacco (Goldberg et al. 1993, 1995; Beals and Goldberg 1997; Sanders et al. 2005), tomatoes (Bonner and Dickinson 1989; Senatore et al. 2009), and *Solanum* species (Garcia et al. 2008), in which the stomium region is also comprised of the septum and stomium. In Solanaceae species, the specialized cells under the stomium were referred to as circular cell cluster. Anthers of most non-solanaceous species do not have a circular cell cluster, but have specialized septum cells under the stomium, functioning analogously in dehiscence. The basic process of anther opening among the dicot model plant *A. thaliana*, the Solanaceae, and the monocots rice and maize is that began with the degeneration of specialized septum cells uniting the two microsporangia of each theca into a confluent chamber, and followed by the split of the stomium cells shedding the pollen grains. In *P. trimera*, the anther dehiscence mode could be expected that the anther septum and stomium go through a process of cell death and degeneration to facilitate pollen release at flower opening, which is similar to the dicot model plant *A. thaliana*, the Solanaceae, and to the monocots rice and maize, and it supports that the basic process of anther dehiscence appears conserved across different plant species (Beals and Goldberg 1997; Kuriyama and Fukuda 2002; Sanders et al. 2005; Senatore et al. 2009; Wilson et al. 2011). However,

staminodes from hermaphroditic flowers do not dehisce at anthesis, due to a nonfunctional stomium region, i.e. both cells of the septum (two layers) and stomium (1–3 modified epidermal cells) persist and keep intact. Delayed dehiscent staminode was observed in *P. mulgraveana* by Pang et al. (2013), but indehiscent staminode or delayed dehiscent outer stamen has not been reported previously in the Annonaceae and other angiosperm plants. However, either failing to dehisce or defection in the timing of anther dehiscence have been identified in a large number of *A. thaliana* male-sterile dehiscence mutants (Dawson et al. 1993, 1999; Sanders et al. 1999, 2000; Stintzi and Browse, 2000; Ishiguro et al. 2001; Park et al. 2002; Von Malek et al. 2002; Steiner Lange et al. 2003) and analogous tobacco mutants (Goldberg et al. 1993; Beals and Goldberg 1997). Beals and Goldberg (1997) reported that a functional stomium is required for anther dehiscence regardless of the viability of pollen grains. Anther dehiscence is not simply a mechanical process, but involves specific, exquisitely timed, cellular events.

Sexual differentiation of flowers

Unisexual flowers of the great majority of monoecious and dioecious plants often undergo a hermaphroditic stage at early stages of development. Both sexual organs are initiated at this stage, but one of the sex organs loses its functions because of

development arrest or selective abortion at a crucial developmental stage, varying from the appearance of primordia of reproductive organs, to the formation of completely developed but non-functional organs (Dellaporta and Calderon-Urrea 1993; Mitchell and Diggle 2005). Given the wide variety of stages of arrest of reproductive organs, it is a widely held opinion that to analyze the developmental changes that have occurred during the evolution of unisexual flowers a detailed morphological analysis is important and necessary. In *P. trimera*, the gender difference appears in morphology at the stage when the first whorl of six reproductive organs is initiated. After the appearance of the first three paired stamen primordia in staminate flowers, additional 40–50 stamen primordia arise centripetally toward the top of the floral apex and occupy the entire floral apex. Any evidence of carpel primordia initiation or abortion could not be found during the whole developmental stage. It indicates that staminate flower in *P. trimera* is unisexual from inception and does not go through a hermaphroditic stage. In pistillate flowers, 9–15 carpels arranged in two whorls develop rapidly at the center of the floral apex after the first whorl of staminode primordia initiation. As the development of the carpels, the staminodes develop normally and differentiate into microsporangia, containing tetrads similar in morphology as in the stamens from staminate flowers. The differentiation of

microsporangia and filament are similar between the stamens in staminate flower and staminodes in pistillate flowers during the floral development, except that the number of staminode primordia arranges from 3 to 6 after initiation of the first whorl of carpel primordia. Although some staminode primordia disappear, the remaining staminodes are 3–6, well developed and arrange in a whorl opposite the outer petals. The androecium with three stamens forming an outermost whorl was observed in *Orophea* (Kessler 1988). In this case, the pistillate flowers could be morphologically recognized as hermaphroditic flowers, and *P. trimera* is structurally andromonoecious.

Inner staminodes were reported in Magnoliales, such as in Eupomatiaceae, Himantandraceae, Degeneriaceae (Endress 1984), and some species of *Anaxagorea* and *Xylopia* in Annonaceae (van Heusden 1992; Scharaschkin and Doyle 2005, 2006; Endress and Doyle 2009; Endress and Armstrong 2011). Outer staminodes were more commonly observed in Annonaceae, e.g. some species of *Monanthotaxis* (Ronse De Craene and Smets 1990), *Miliusa* (Narayanan et al. 2010), *Uvaria* (van Heusden 1992; Xu and Ronse De Craene 2010), and also appeared in Magnoliaceae (e.g. *Woonyoungia*) (FU et al. 2009). All these staminodes were reported in lacking microsporangia. Most species of *Pseuduvaria* (only two species have solely hermaphroditic flowers) are known to have unisexual flowers (Pang et al. 2013),

either being structurally andromonoecious (or androdioecious), or monoecious (or dioecious), and outer staminodes were only found in flowers that were regarded as functionally pistillate (Su and Saunders 2006; Su et al. 2008, 2010). These outer staminodes were considered either lack pollen grains or else produce sterile pollen grains as the grains are smaller than the corresponding fertile pollen grains. In this study, staminodes in hermaphroditic flowers contain 2–4 short microsporangia with tetrads which are similar to that of fertile stamens in shapes, size, and ornamentation of exine. Although the resolution of the pollen viability is beyond the scope of this study, morphological and structural features reveal that these staminodes are indehiscent at anthesis resulting in failure of the pollen grains release, and hence preclude transfer of pollen grains from hermaphroditic flowers. The morphologically hermaphroditic flowers are therefore functionally pistillate, and the structural andromonoecy of *P. trimera* actually functions as true monoecy.

In addition, the androecium in staminate flower dehisces and abscises centrifugally, with stamens at the center of the androecium dehiscing and abscising previously than those at the margin, and the outer stamens are morphologically and structurally similar to the staminodes in 2–4 short microsporangia. Delayed anther dehiscence, added to the asymmetrical shape (3 microsprangia differed in length) in

the outer stamen, indicates that the inner stamens are selectively advantageous in releasing pollens, while the outer stamens act as substitutes for the continued availability of pollen grains. In this case, the outer stamen from *P. trimera* probably has a tendency towards being sterile via a delayed anther dehiscence. Analogous phenomenon that stamens of structurally hermaphroditic flowers with fertile pollens become sterile due to the delayed anther dehiscence in *P. mulgraveana* was reported by Pang et al. (2013). The mechanism to achieve functional unisexual flowers (monoecy) in *P. mulgraveana* is likely to effectively promote xenogamy: the opportunities for intra-individual pollen transfer are reduced, limiting the possibility of geitonogamy. Considering the similar mechanism of sterility via delayed dehiscent anther or indehiscent anther to achieve functionally unisexual flowers in *P. trimera* and *P. mulgraveana*, and the widespread presence of staminodes in functionally pistillate flowers in *Pseuduvaria* (Su and Saunders 2006; Saunders 2010), it could infer that the occurrence of staminode is closely correlated with the acquisition and evolution of functional unisexual flowers in the genus *Pseuduvaria*. The occurrence of functionally unisexual flowers is to support outbreeding, which is relatively frequent among basal angiosperms (Gottsberger 2016).

Conclusions

Two sheathing bracts are present at the early floral development. Floral phyllotaxis of *P. trimera* corresponds with other studied Annonaceae species in complex whorled phyllotaxis with double positions in the first stamen whorl (staminate flower) or staminode whorl (pistillate flower). The septum and stomium cells from stamens break down developmentally and facilitate anther dehiscence and tetrads release at anthesis, whereas those in staminodes maintain intact producing indehiscent anthers. The morphologically hermaphrodictic flowers in *P. trimera* become functionally pistillate flowers due to indehiscent staminodes, and therefore functionally monoecious. This mechanism to achieve functional unisexuality flowers is coincident with the species of *P. mulgraveana* (Pang et al. 2013). The outer stamens are morphologically similar to the staminodes with decreased length and number of microsporangia and tend to be sterile via a delayed anther dehiscence, aiming to effectively prevent geitonogamy.

Acknowledgements

We acknowledge Senior Engineer Xiao-Ying Hu (South China Botanical Garden, Chinese Academy of Sciences) for support with SEM and Junior Ru-Fang Deng for support with semi-thin sectioning. We thank the National Natural Science Foundation

of China (NSFC) (Grant No.31270227) and the Knowledge Innovation Program of the Chinese Academy of Sciences (Grant No.KSCX2-EW-J-28) for financial support.

References

Armstrong JE, SC Tucker 1986 Floral development in *Myristica* (Myristicaceae). Am J Bot 73: 1131–1143.

Beals TP, RB Goldberg 1997 A novel cell ablation strategy blocks tobacco anther dehiscence. Plant Cell 9:1527–1545.

Bonner LJ, HG Dickinson 1989 Anther dehiscence in *Lycopersicon esculentum Mill.* I. Structural aspects. New Phytol 113: 97–115.

Couvreur TLP, MD Pirie, LW Chatrou, RMK Saunders, YCF Su, JE Richardson, RHJ Erkens 2011 Early evolutionary history of the flowering plant family Annonaceae: steady diversification and boreotropical geodispersal. J Biogeogr 38: 664–680.

Dawson J, E Sözen, I Vizir, SV Waeyenberge, ZA Wilson, BJ Mulligan 1999 Characterization and genetic mapping of a mutation (*ms35*) which prevents anther dehiscence in *Arabidopsis thaliana* by affecting secondary wall thickening in the endothecium. New Phytol 144: 213–222.

Dawson J, ZA Wilson, MGM Aarts, AF Braithwaite, LG Briarty, BJ Mulligan 1993

Microspore and pollen development in six male-sterile mutants of *Arabidopsis thaliana*. Can J Bot 71:629–638.

Dellaporta SL, A Calderon-Urrea 1993 Sex determination in flowering plants. Plant Cell 5:1241–1251.

Endress PK 1984 The role of inner staminodes in the floral display of some relic Magnoliales. Plant Syst Evol 146: 269–282.

— — — 2003 Early floral development and the nature of the calyptra in Eupomatiaceae. Int J Plant Sci 164: 489–503.

Endress PK, JE Armstrong 2011 Floral development and floral phyllotaxis in *Anaxagorea* (Annonaceae). Ann Bot 108: 835–845.

Endress PK, JA Doyle 2007 Floral phyllotaxis in basal angiosperms –development and evolution. Curr Opin Plant Biol 10: 52–57.

— — — 2009 Reconstructing the ancestral angiosperm flower and its initial specializations. Am J Bot 96: 22–66.

Fu L, QW Zeng, JP Liao, F Xu 2009 Anatomy and ontogeny of unisexual flowers in dioecious *Woonyoungia septentrionalis* (Dandy) Law (Magnoliaceae). J Syst Evol 47: 263–272.

Garcia CC, M Matesevach, G Barboza 2008 Features related to anther opening in *Solanum* species (Solanaceae). Bot J Linn Soc 158: 344–354.

Goldberg RB, TP Beals, PM Sanders 1993 Anther development: basic principles and practical applications. Plant Cell 5: 1217–1229.

Goldberg RB, PM Sanders, TP Beals 1995 A novel cell-ablation strategy for studying plant development. Phil Trans R Soc Lond B 350: 5–17.

Gottsberger G 2016 Generalist and specialist pollination in Basal angiosperms (ANITA grade, basal monocots, magnoliids, Chloranthaceae and Ceratophyllaceae): what we know now. Plant Div Evol Vol 131: 263–362.

Ishiguro S, A Kawai-Oda, J Ueda, I Nishida, K Okada 2001 The *DEFECTIVE IN ANTHER DEHISCENCE* gene encodes a novel phospholipase A1 catalyzing the initial step of jasmonic acid biosynthesis, which synchronizes pollen maturation, anther dehiscence, and flower opening in Arabidopsis. Plant Cell 13: 2191–2209.

Keijzer CJ, HB Leferink-Ten Klooster, MC Reinders 1996 The mechanics of the grass flower: anther dehiscence and pollen shedding in maize. Ann Bot 78: 15–21.

Kessler PJA 1988 Revision der *Gattung Orophea* Blume (Annonaceae). Blumea 33: 1–80.

Kim S, J Koh, H Ma, Y Hu, PK Endress, Hauser BA, M Buzgo, PS Soltis, DE Soltis 2005 Sequence and expression studies of A-, B-, and E-class MADS-box genes in *Eupomatia* (Eupomatiaceae): support for the bracteates origin of the calyptra. Int J Plant Sci 166: 185–198.

Kuriyama H, H Fukuda 2002 Developmental programmed cell death in plants. Curr Opin Plant Biol 5: 568–573.

Matsui T, K Omasa, T Horie 1999 Mechanism of anther dehiscence in rice (*Oryza sativa L.*). Ann Bot 84: 501–506.

Mitchell CH, PK Diggle 2005 The evolution of unisexual flowers: morphological and functional convergence results from diverse developmental transitions. Am J Bot 92: 1068–1076.

Narayanan MKR, P Sujanapal, NA Kumar, N Sasidharan, M Sivadasan 2010 *Miliusa wayanadica* (Annonaceae), a new species from Western Ghats, India. J Bot Res Inst Texas 4: 63–67.

Pang CC, T Scharaschkin, YCF Su, RMK Saunders 2013 Functional Monoecy Due to Delayed Anther Dehiscence: A Novel Mechanism in *Pseuduvaria mulgraveana* (Annonaceae). Plos One 8: e59951.

Park JH, R Halitschke, HB Kim, IT Baldwin, KA Feldmann, R Feyereisen 2002 A knock-out mutation in allene oxide synthase results in male sterility and defective wound signal transduction in Arabidopsis due to a block in jasmonic acid biosynthesis. Plant J 31: 1–12.

Ronse De Craene LP, E Smets 1990 The floral development of *Popowia whitei* (Annonaceae). Nord J Bot 10: 411–420.

Sanders PM, AQ Bui, BH Le, RB Goldberg 2005 Differentiation and degeneration of cells that play a major role in tobacco anther dehiscence. Sex Plant Reprod 17: 219–241.

Sanders PM, AQ Bui, K Weterings, KN McIntire, YC Hsu, PY Lee, MT Truong, TP Beals, RB Goldberg 1999 Anther developmental defects in *Arabidopsis thaliana* male-sterile mutants. Sex Plant Reprod 11: 297–322.

Sanders PM, PY Lee, C Biesgen, JD Boone, TP Beals, EW Weiler, RB Goldberg 2000 The Arabidopsis *DELAYED DEHISCENCE1* gene encodes an enzyme in the jasmonic acid synthesis pathway. Plant Cell 12: 1041–1061.

Saunders RMK 2010 Floral evolution in the Annonaceae: hypotheses of homeotic mutations and functional convergence. Biol Rev 85: 571–591.

Scharaschkin T, JA Doyle 2005 Phylogeny and historical biogeography of *Anaxagorea* (Annonaceae) using morphology and non-coding chloroplast sequence data. Syst Bot 30: 712–735.

——— 2006 Character evolution in *Anaxagorea* (Annonaceae). Am J Bot 93: 36–54.

Senatore A, CP Trobacher, JS Greenwood 2009 Ricinosomes predict programmed cell death leading to anther dehiscence in tomato. Plant Physiol 149: 775–790.

Steiner-Lange S, US Unte, L Eckstein, C Yang, ZA Wilson, E Schmelzer, K Dekker, H Saedler 2003 Disruption of *Arabidopsis thaliana* MYB26 results in male

sterility due to non-dehiscent anthers. Plant J 34: 519–528.

Stintzi A, J Browse 2000 The Arabidopsis male-sterile mutant, *opr3*, lacks the 12-oxophytodienoic acid reductase required for jasmonate synthesis. PNAS 97: 10625–10630.

Su YCF, T Chaowasku, RMK Saunders 2010 An extended phylogeny of *Pseuduvaria* (Annonaceae) with descriptions of three new species and a reassessement of the generic status of *Oreomitra*. Syst Bot 35: 30–39.

Su YCF, RMK Saunders 2006 Monograph of *Pseuduvaria* (Annonaceae). Syst Bot Monogr 79: 1–204.

Su YCF, GJD Smith, RMK Saunders 2008 Phylogeny of the basal angiosperm genus *Pseuduvaria* (Annonaceae) inferred from five chloroplast DNA regions, with interpretation of morphological character evolution. Mol Phylogenet Evol 48: 188–206.

van Heusden ECH 1992 Flowers of Annonaceae: morphology, classification, and evolution. Blumea **7**: 1–218.

von Malek B, E van der Graaff, K Schneitz, B Keller 2002 The Arabidopsis male-sterile mutant *dde2-2* is defective in the *ALLENE OXIDE SYNTHASE* gene encoding one of the key enzymes of the jasmonic acid biosynthesis pathway. Planta 216: 187–192.

Wilson ZA, J Song, B Taylor, C Yang 2011 The final split: the regulation of anther dehiscence. J Exp Bot 62: 1633–1649.

Xu F, LP Ronse De Craene 2010 Floral ontogeny of Annonaceae: evidence for high variability in floral form. Ann Bot 106: 591–605.

Figure legends

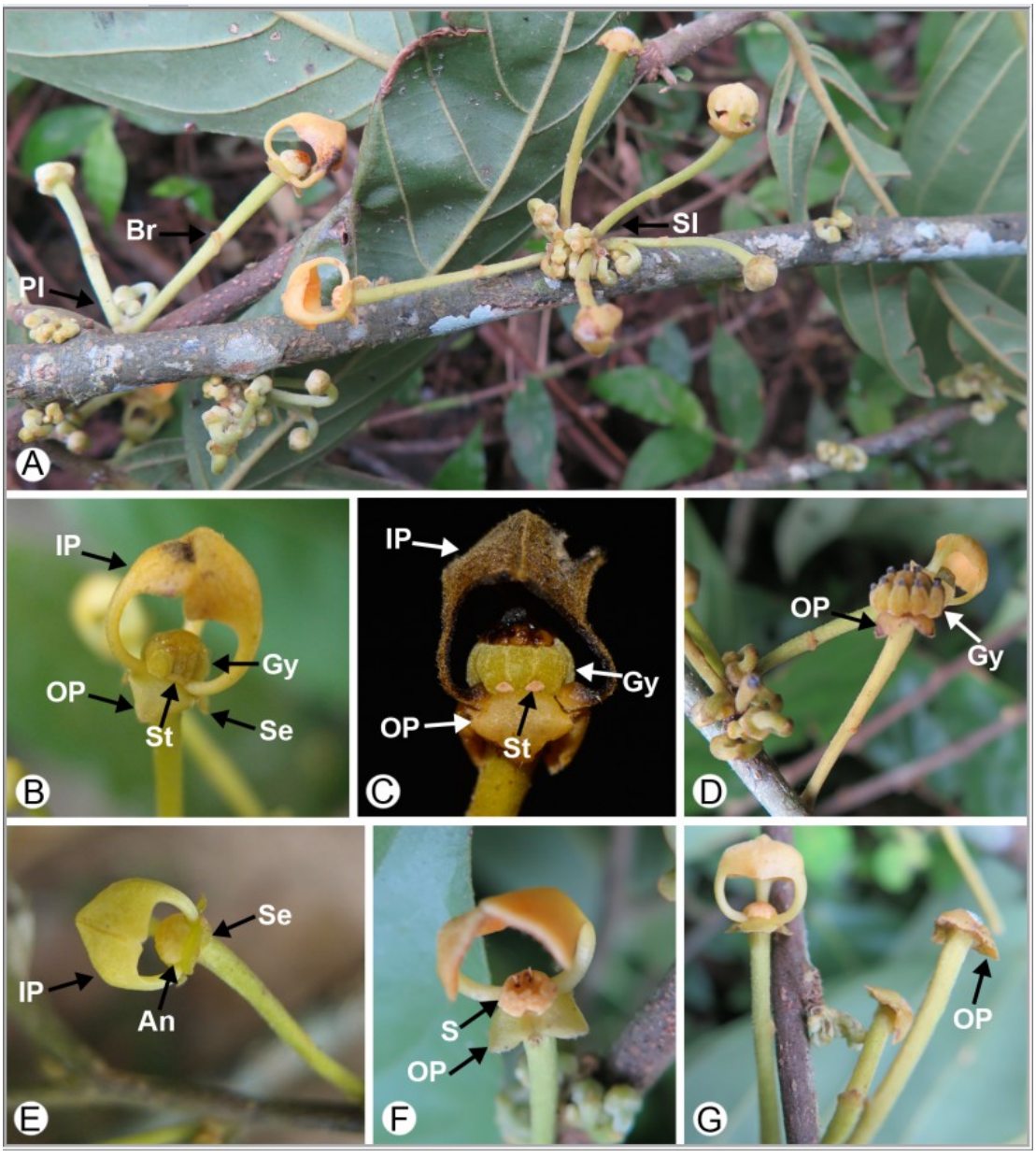

Fig. 1 Flower morphology at anthesis in *Pseuduvaria trimera*. *A*, A twig with

staminate and pistillate inflorescences, at varying developmental stages of flower buds. *B–D* Pistillate flowers. *B*, Sexually mature pistillate flower, showing receptive stigmas with exudate and intact staminodes. *C*, Mitriform inner petal whorl starting to abscise as a whole, and the stigmas becoming dry and no more receptive; the staminodes remain indehiscent; front inner petal was removed. *D*, Later stage with persistent outer petals and the shrunk black stigmas. *E–G*, Staminate flowers. *E*, Immature flower with compact stamens. *F*, Sexually mature staminate flower, with inner whorls of anthers dehiscing and shedding centrifugally. *G*, Outer petals persist after abscission of stamens and mitriform inner petal whorl. An = androecium; Br = bract; Gy = gynoecium; IP = inner petal; OP = outer petal; PI = pistillate inflorescence; S = stamen; Se = sepal; SI = staminate inflorescence; St = staminode.

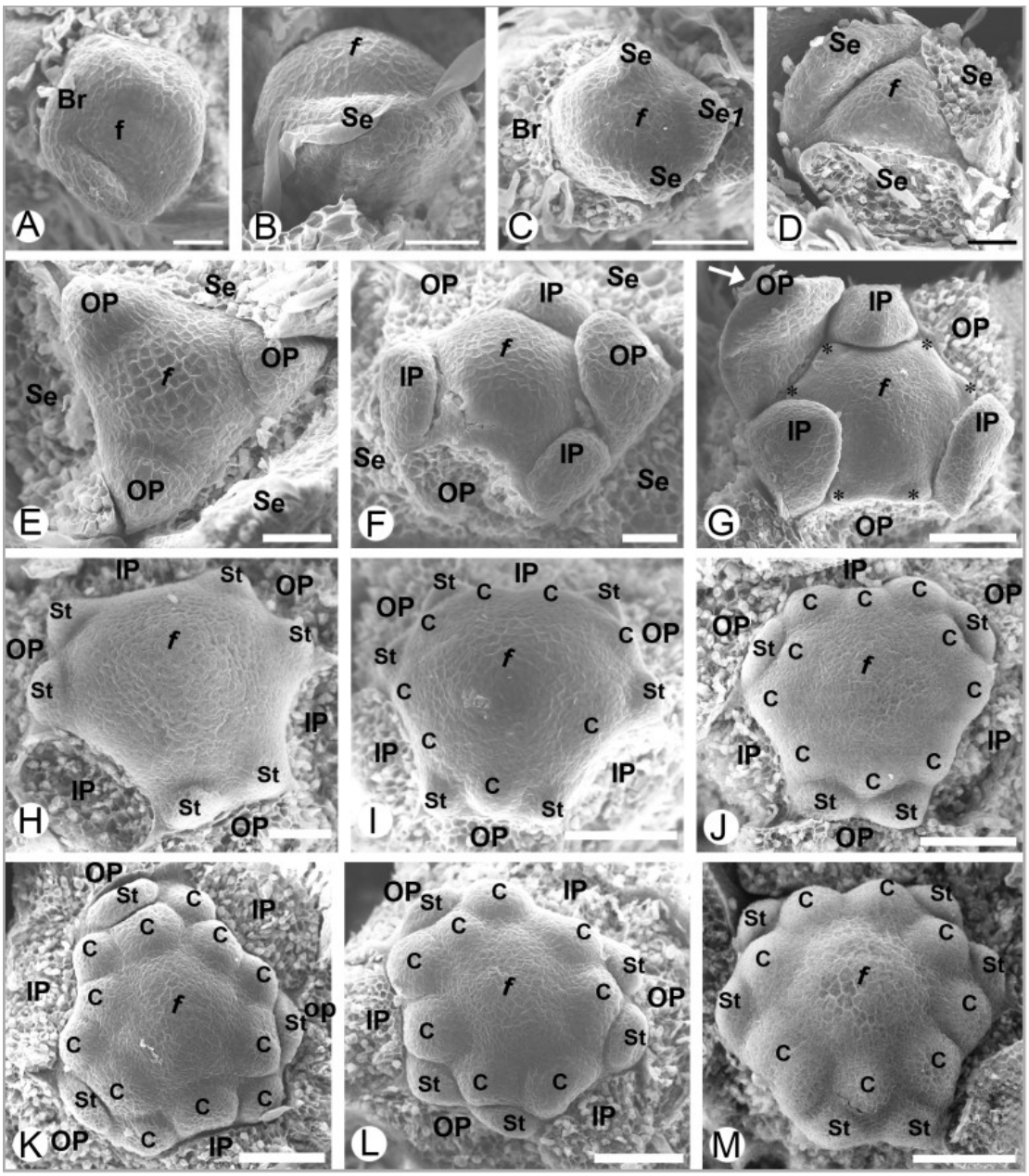

Fig. 2 Early stages of floral development in pistillate *Pseuduvaria trimera*. *A*, Initiation of a bract primordium surrounding the floral apex. *B–D*, Sequential initiation of the whorl of sepal primordia; the first sepal primordium (marked with *Se1*), opposite the sheathing bract (removed); the floral apex becomes triangular. *E*, The second whorl of three outer petal primordia is initiated at the tips of the three

angles of the triangular floral apex. *F*, The third whorl of three inner petal primordia appears, alternating with the outer petal primordia; the floral apex becomes hexagonal. *G*, A whorl of staminode primordia (marked with *asterisks*) arises as three pairs, opposite the outer petals; hairs present on the back of the outer petals (marked with *arrow*). *H*, Later stage with three pairs of slightly larger staminode primordia (all perianth members were removed). *I*, *J*, Initiation of the first whorl of carpel primordia. *K–M*, Slightly older stage showing larger carpel primordia; number of the carpel primordia is fluctuating: eight in *L*, *M*, ten in *J*, twelve in *K*; number of the staminode primordia becoming six (*I*, *M*), four (*J*), three (*K*), five (*L*), either in single or double positions. *A–M*, Top views. Br = bract; C = carpel; f = floral apex; IP = inner petal; OP = outer petal; Se = sepal; Se1= the first sepal; St = staminode. Scale bars: *A*, *D*, *E*, *H* = 50 μm; *B*, *C*, *G*, *I–M* = 100 μm.

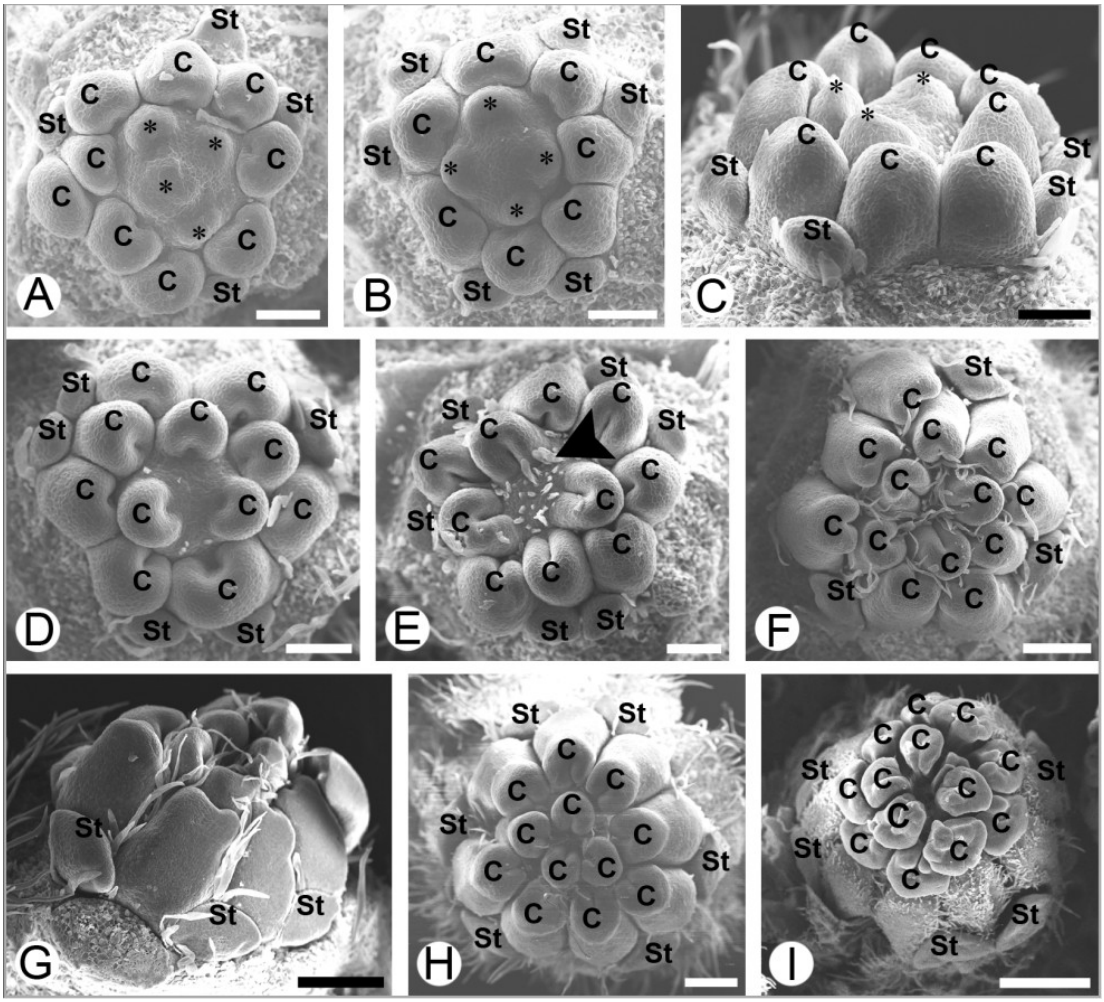

Fig. 3 Older stages of floral development of pistillate *Pseuduvaria trimera*. *A–C*, Initiation of the second whorl of carpel primordia (marked with *asterisks*): three in *C* and four in *A*, *B*; the first whorl of carpel primordia becoming horseshoe-shaped and more enlarging than outer staminode primordia; *C*, Lateral view showing the staminode primordia without microsporangia. *D*, A depression appears on the ventral surface of each carpel and all carpel primordia become horseshoe-shaped. *E*, The ventral depression deepens, extending to the tip of each carpel, and hairs (marked with *arrowhead*) appear on the remaining floral apex. *F–I*, Comparative development of

the gynoecium and staminodes. *F*, Carpels become conduplicate and hairs grow between the carpels. *G*, Lateral view (about the similar stage as in *F*), showing bulging microsporangia in staminodes. *H*, Carpels closing and plicating, note the formation of stigma heads and bulging ovaries. *I*, Mature gynoecium, showing folded and funnel-shaped stigma heads and deeply hairy ovaries. *A*, *B*, *D–F*, *H*, *I*, Top views; *C*, *G*, Lateral views. C = carpel; St = staminode. Scale bars: *A–E* = 100 μm; *F–H* = 200 μm; *I* = 500 μm.

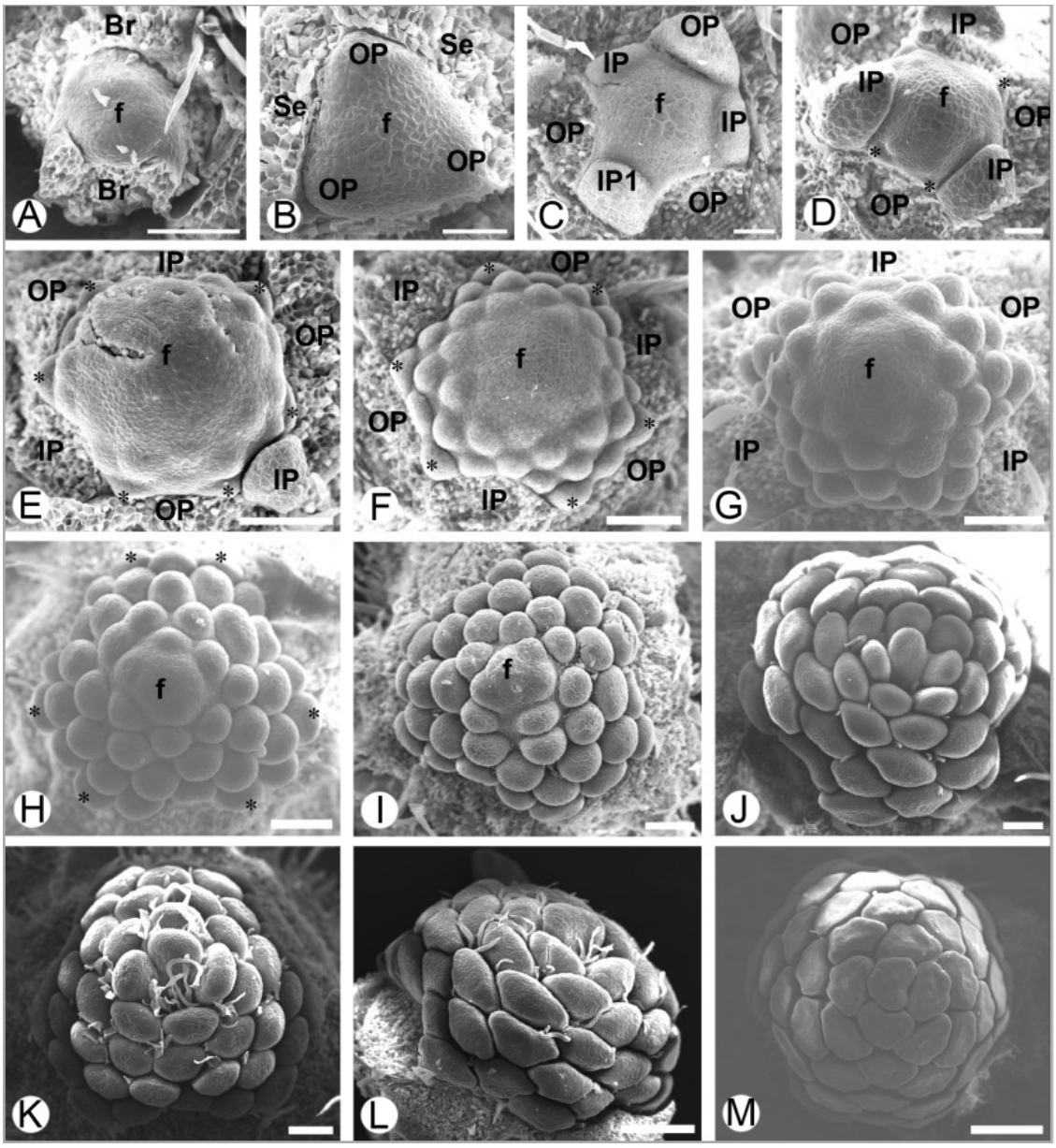

Fig. 4 Floral development of staminate *Pseuduvaria trimera*. *A*, Young flower bud with two sheathing bracts (removed). *B*, Initiation of the second whorl of outer petal primordia. *C*, Initiation of the third whorl of inner petal primordia; one of the inner petals (marked with *IP1*) is slightly larger than the other two. *D*, Initiation of the first whorl of stamen primordia (marked with *asterisk*), opposite the outer petals; hairs grow on the back of the inner petals and the floral apex becomes high and large. *D–G*,

Centripetal initiation of the additional stamens. *H–J*, Initiation of the innermost stamen primordia. *H*, Floral apex surrounding by six stamen primordia. *I*, Smaller floral apex surrounded by three stamen primordia. *J*, Floral apex is occupied at last by a unique stamen primordium. *K–M*, Further development of the androecium. *K*, Hairs are growing among the stamen primordia. *L*, Lateral view of the androecium, showing the bulging microsporangia in stamens. *M*, Mature androecium, containing compact stamens with one topmost stamen and expanded connective appendage. Br = bract; f = floral apex; IP = inner petal; IP1= the first inner petal; OP = outer petal; Se = sepal. Scale bars: *B–D* = 50 μm; *A*, *E–K* = 100 μm; *L* = 200 μm; *M* = 500 μm.

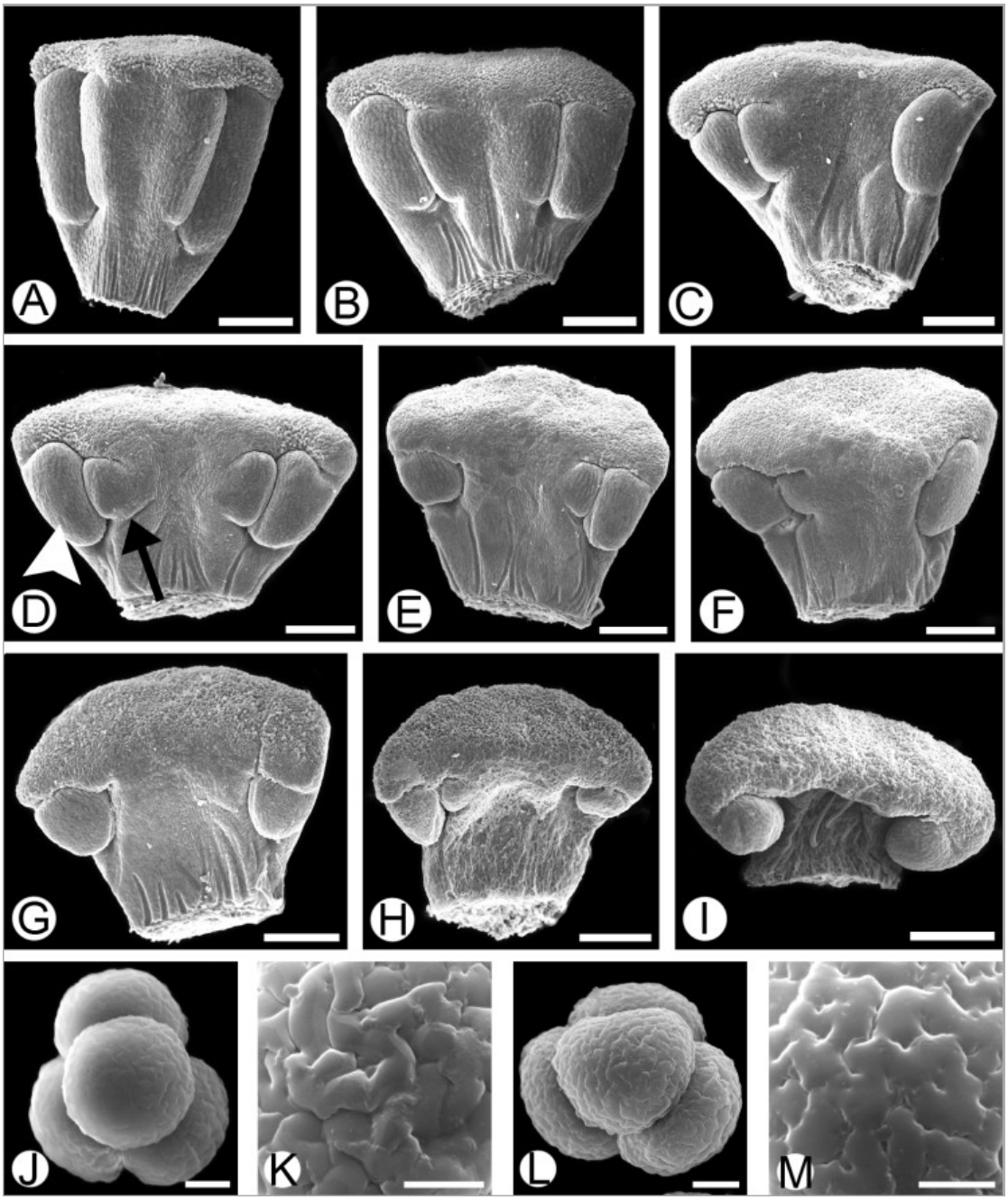

Fig. 5 Comparative morphology between stamens and staminodes, and their tetrads at anthesis in *Pseuduvaria trimera*. *A*, Stamen from the inner whorls of the androecium comprises two pairs of pollen sacs; paired pollen sacs differ slightly in length. *B*, *C*, Stamens from the outer whorls of the androecium, comprise four (*B*) or three (*C*)

conspicuously shorter pollen sacs. *D*, Staminode with four short pollen sacs; obviously inequal, with the outer one (marked with *arrowhead*) being much larger than the inner (marked with *arrow*). *E*, *F*, Staminodes with three short pollen sacs. *G*, Staminode with two short pollen sacs. *H*, *I*, Shrunk staminodes contain either three or two indehiscent pollen sacs. *J*–*M*, Representative pollen tetrad shapes and detail of exinic microrugulate ornamentations. *J*, *K*, In stamen. *L*, *M*, In staminode. Scale bars: *A*–*I* = 200 μm; *J*, *L* = 10 μm; *K*, *M* = 5 μm.

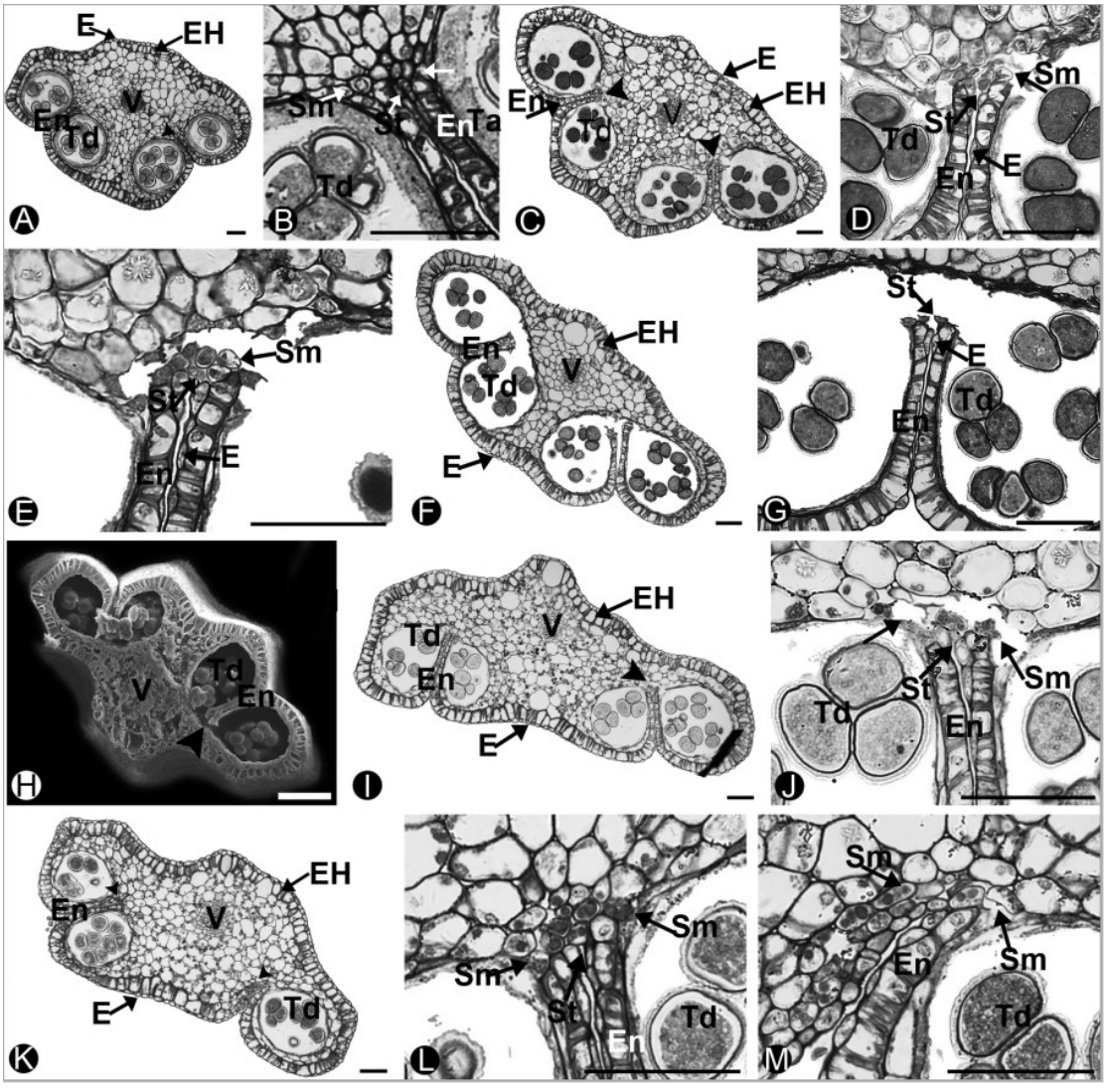

Fig. 6 Comparative stamen histology at maturity in *Pseuduvaria trimera*. *A*, *C*, *F*, *H*, Cross sections of the stamens from the inner whorls of the androecium, showing one vascular bundle, the epidermis layer, the U-shaped-thickened endothecium and the endothecial-like cells, surrounding the pollen sacs and the entire connective tissue, tetrads, and the stomium regions between the paired pollen sacs (marked with *arrowhead*). *B*, *D*, *E*, *G*, Details of cells in the stomium region from *A*, *C*, *F*: *B*, Stomium region from the stamen in *A*, is composed of a layer of septum cells and several of stomium cells; *D*, *E*, Septum cells of the stomium region from *C* break down and separate from the connective tissues, but some of them remain in close contact and intact; the stomium cells also keep intact; *G*, Anther wall separates from the connective tissue, forming a locule theca; the stomium cells break down. *H*, Cross sectioned anther (SEM), showing microsporangia with tetrads. *I*, *K*, Cross sections of stamens from the outer androecial whorl. *I*, Stamen with four pollen sacs. *J*, Details of cells in the stomium region from *I*, showing the disrupting septum cells and the intact stomium cells. *K*, Stamen with three pollen sacs. *L*, *M*, Details of cells in the stomium region from *K*: *L*, Stomium region between paired pollen sacs, comprising a layer of septum cells and several stomium cells; *M*, Stomium region of single pollen sac, consisting of two layers of septum cells and several stomium cells; the septum cells

start to break down. E = epidermis; EH = endothecial-like connective hypodermis; En = endothecium; Sm = septum; St = stomium; Ta= tapetum; Td = tetrad; V = vascular bundle. Scale bars: *A–G*, *I–M* = 50 μm; *H* =100 μm. All *arrowheads* point to the position of stomium region.

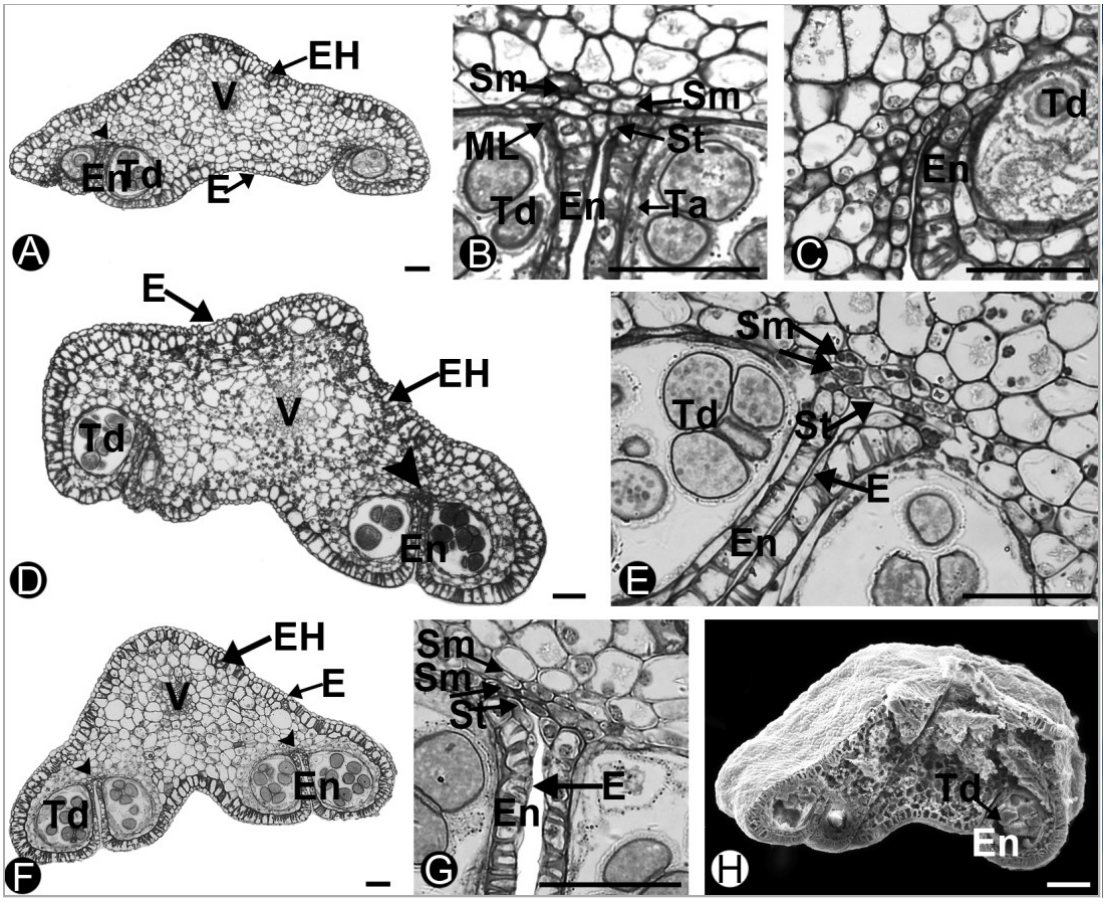

Fig. 7 Comparative Anatomies of staminode histology at maturity in *Pseuduvaria trimera*. *A*, Cross section of anther from preanthetic flower bud, showing one vascular bundle, three pollen sacs with tetrads, and the U-shaped-thickened endothecium and the endothecial-like cells. *B*, *C*, Details of cells in the stomium region in *A*: *B*, Stomium region between paired pollen sacs, showing two layers of compressed

septum cells and several stomium cells; *C*, Note the single pollen sac devoid of any stomium region. *D*, *F*, Transverse sections of staminodes at anthesis, showing one vascular bundle, two pairs of pollen sacs with tetrads, the U-shaped-thickened endothecium and endothecial-like cells, surrounding the pollen sacs and the entire connective tissue. *E*, *G*, Details of cells in the stomium region in *D*, *F*, respectively: note three layers of intact septum and stomium cells between adjacent pollen sacs. *H*, Cross sectioned staminode at anthesis, showing three pollen sacs enclosing tetrads. E = epidermis; EH = endothecial-like connective hypodermis; En = endothecium; ML = middle layer; Sm = septum; St = stomium; Ta = tapetum; Td = tetrad; V = vascular bundle. Scale bars: *A*–*G* = 50 μm; *H* = 100 μm. All *arrowheads* point to the position of stomium region.